Mechanical Systems and Signal Processing 178 (2022) 109150

Contents lists available at ScienceDirect

Mechanical Systems and Signal Processing

journal homepage: www.elsevier.com/locate/ymssp

# Simulation of non-stationary and non-Gaussian random processes by 3rd-order Spectral Representation Method: Theory and POD implementation

Lohit Vandanapu, Michael D. Shields *

*Johns Hopkins University, Baltimore, United States*

ARTICLE INFO

Communicated by I. Kougioumtzoglou

*Keywords:*
Random process
Spectral representation
Non stationary
Fast Fourier Transform
Proper Orthogonal Decomposition

ABSTRACT

This paper introduces the 3rd-order Spectral Representation Method for simulation of non-stationary and non-Gaussian stochastic processes. The proposed method extends the classical 2nd-order Spectral Representation Method to expand the stochastic process from an evolutionary bispectrum and an evolutionary power spectrum, thus matching the process completely up to third-order. A Proper Orthogonal Decomposition (POD) approach is further proposed to enable an efficient FFT-based implementation that reduces computational cost significantly. Two examples are presented, including the simulation of a fully non-stationary seismic ground motion process, highlighting the accuracy and efficacy of the proposed method.

## 1. Introduction

Monte Carlo Simulation of non-stationary stochastic processes is of extreme importance, especially for simulation of extreme events like earthquake ground motion or transient wind gusts. These simulations are particularly essential in the case of structural systems involving non-linear dynamics where uncertainity cannot be quantified analytically.

Properties of a stationary process remain the same at every instant of time and because to this independence in frequency and time, computationally efficient methods for the simulation of stationary process can be derived. On the other hand the properties of a non-stationary process vary with time making their simulation challenging because this introduces dependence between time and frequency. For the simulation of stationary stochastic processes, the Spectral Representation Method (SRM) and Karhunen–Loeve Expansion (KLE) [1] are the most widely-used methods. Both methods rely on an expansion of a random process having a truncated form:

$$X(t) \approx \sum_{i=1}^{N} \theta_i(\omega)\psi_i(t) \tag{1}$$

where $\psi(t)$ are orthogonal basis functions and $\theta(\omega), \omega \in \Omega$ are random variables. The primary difference between SRM and KLE is that SRM uses harmonic basis functions, whereas KLE uses the eigenfunctions of the covariance function as the basis functions. In this work, we will focus on novel developments for the SRM.

Shinozuka was the first to use the Spectral Representation Method for the simulation of stochastic processes [2]. Then, Yang [3] suggested the use of Fast Fourier Transform (FFT) to improve its computational efficiency. The complete theoretical footing for the SRM was then established in the 1990s along with extensions for the simulation of ergodic vector processes [4], stochastic waves [5], random fields [6].

* Corresponding author.
*E-mail addresses:* lvandan2@jhu.edu (L. Vandanapu), michael.shields@jhu.edu (M.D. Shields).

https://doi.org/10.1016/j.ymssp.2022.109150
Received 12 October 2021; Received in revised form 25 March 2022; Accepted 7 April 2022
Available online 16 May 2022

Samples generated by the SRM are Gaussian (either naturally or asymptotically depending on the implementation [7]). This is convenient for many applications, but limiting for applications involving non-Gaussian (i.e. higher-order) stochastic processes. To fill this gap, several methods for the simulation of non-Gaussian processes have been proposed. One class of such methods works by introducing correlated random variable with deterministic basis functions like Hermite and Legendre polynomials [8,9]. Another class of processes works by performing an inverse Cumulative Distribution Function (CDF) transform of Gaussian samples [10] referred to as the 'translation' process as

$$Y(t) = F^{-1}(\Phi(X(t))) \tag{2}$$

where $X(t)$ is a standard Gaussian stochastic process, $\Phi(\cdot)$ is the standard normal CDF and $F(\cdot)$ is the CDF of the non-Gaussian distribution. A wide range of methods utilizing translation process theory have been developed [11–13]. More recently, a class of methods has been developed that theoretically extends the SRM to higher-order ($3^{\text{rd}}$-order asymmetrically non-Gaussian) stochastic processes by considering interactions among the wave components of the SRM expansion [14,15].

The SRM for simulation of non-stationary stochastic processes was also presented in the seminal paper by Shinozuka [2] and relies on the theory of evolutionary power developed by Priestley [16]. But the formula was based on the summation of the trigonometric cosines functions which is computationally inefficient. To improve the efficiency of the simulation process, Li and Kareem [17] proposed the use of discrete fourier transform in tandem with digital filtering. Huang [18] also developed FFT-aided methods involving the use of wavelets. All these methods focused only on using FFT directly on the evolutionary power spectrum. But, additional savings can be obtained by projecting the evolutionary power spectrum onto a lower-dimensional orthogonal basis in the frequency domain and considering time varying modulations of the corresponding components. This has the effect of decomposing the non-stationary process into the sum of time–frequency separable processes in which each process has a stationary component that is modulated in time. Li and Kareem [19] suggested the use of orthogonal legendre polynomials to decompose the evolutionary spectrum and established an FFT-aided spectral representation method. Huang [20] proposed an FFT-based approach that leverages the Proper Orthogonal Decomposition (POD) for the simulation of multivariate processes. POD was also used in conjunction with Stochastic wave theory in the simulation of multivariate non-stationary random processes [21]. The POD involves projecting high-dimensional data (i.e. the evolutionary spectrum) onto to a low-dimensional manifold by finding the best set of basis functions. Since most of the information is contained within a few modes, the POD can drastically reduce the dimensionality of the data. For SRM-based simulations this drastically reduces computation cost.

Simulation of non-stationary and non-Gaussian random processes compounds the challenges of simulating non-Gaussian processes with those of simulating non-stationary processes. As a result, few methods have been developed to successfully simulate these complex processes [13,22–27]. Those that use the SRM for simulation, rely on an expansion from the evolutionary spectrum coupled with translation process theory [13,23,24]. Here, we derive a direct third-order SRM from the evolutionary power spectrum and the evolutionary bispectrum for the simulation of non-Gaussian stochastic processes having known second and third-order properties. This method extends the third-order SRM previously developed for stationary random processes [14], multi-dimensional random fields, and stochastic vector processes [15]. This method can be appropriately combined with multi-dimensional random fields and stochastic vector process proposed in [15] to generate non-stationary vector processes or non-stationary random fields. We further develop a POD-based implementation for the simulations, which allows the use of FFT and drastic computational improvement of the simulation formula. The theoretical properties of the expansion are derived and the effectiveness of the proposed methodology is demonstrated with the use of two numerical examples: one illustrating a simple time–frequency separable third-order process and one considering a non-Gaussian stochastic ground motion process.

## 2. 2nd-order spectral representation for non-stationary stochastic processes

In general, a one-dimensional, uni-variate, zero-mean non-stationary process, $X(t)$, can be expressed as

$$X(t) = \int_{-\infty}^{\infty} \phi(t,\omega) d\,Z(\omega) \tag{3}$$

where $Z(\omega)$ is a spectral process with orthogonal increments having the following properties

$$\begin{aligned} &\mathbb{E}[d\,z(\omega)] = 0 \\ &\mathbb{E}[|d\,z(\omega)|^2] = d\,\mu(\omega) \end{aligned} \tag{4}$$

where $\phi(t,\omega)$ is selected from a suitable family of functions and $\mu(\omega)$ an associated measure such that the covariance function of the process can be expressed as:

$$Cov(X(t), X(s)) = E[X(t)X(s)] = \int_{-\infty}^{\infty} \phi(t,\omega)\phi^*(s,\omega) d\,\mu(\omega). \tag{5}$$

The expression of the stochastic process in Eq. (7) is not unique owing to the fact that $\phi(t,\omega), \mu(\omega)$ can be selected arbitrarily to satisfy Eq. (5). A common selection for stationary stochastic processes is the complex exponentials $\phi(t,\omega) = e^{\imath\omega t}$ such that Eq. (7) admits the classical Cramer spectral representation [28]. The complex exponentials cannot be used for non-stationary processes. Instead, Priestley [16,29] suggested to use the amplitude modulated complex exponentials such that

$$\phi(t,\omega) = A(t,\omega)e^{\imath\omega t}, \tag{6}$$

referred to as an oscillatory process. With this representation, the process is expressed as

$$X(t) = \int_{-\infty}^{\infty} A(t,\omega) e^{\imath\omega t} dz(\omega) \tag{7}$$

and the evolutionary power spectrum can be defined as

$$dS(t,\omega) = |A(t,\omega)|^2 d\mu(\omega) \tag{8}$$

Priestley further suggests that it is convenient to standardize the modulating function such that $A(0,\omega) = 1$, implying that the measure $\mu(\omega) = S(\omega)$ is equal to the power spectrum at time $t = 0$ and $A(t,\omega)$ represents the time change from this original power spectrum. Under these conditions, the two-sided evolutionary power spectral density function is defined as

$$S(t,\omega) = |A(t,\omega)|^2 S(\omega) \tag{9}$$

Given the spectral representation in Eq. (7), Shinozuka [2] showed that the non-stationary process can be simulated by

$$X(t) = \sqrt{2} \sum_{n=0}^{N-1} \sqrt{2S(t,\omega_n)\Delta\omega} \cos(\omega_n t + \Phi_n) \tag{10}$$

where $\Delta\omega$ is the frequency interval, $\Phi_N$ are uniformly distributed random phase angles $\Phi_N \sim Unif[0, 2\pi]$ and $N$ is the total number of frequency intervals used in the expansion with

$$\begin{aligned} \omega_n &= n\Delta\omega \\ \Delta\omega &= \frac{\omega_u}{N}. \end{aligned} \tag{11}$$

and $\omega_u$ is the cutoff frequency. With the evolutionary power spectral density function given in Eq. (9), this simulation equation can be equivalently expressed as:

$$X(t) = \sqrt{2} \sum_{n=0}^{N-1} A(t,\omega_n) \sqrt{2S(\omega_n)\Delta\omega} \cos(\omega_n t + \Phi_n) \tag{12}$$

## 3. 3rd-order spectral representation for non-stationary stochastic processes

In this section, we extend the spectral representation theory to third-order non-stationary stochastic processes. We then present a new expression for the simulation of third-order non-stationary stochastic processes that leverages the spectral representation.

### 3.1. 3rd-order non-stationary spectral representation

The non-stationary spectral representation in Eq. (7) can, in general, be extended to represent stochastic processes of arbitrary order by extending the orthogonality conditions on the spectral process $Z(\omega)$. Extension to third-order introduces the following orthogonality conditions

$$\begin{aligned} &\mathbb{E}[dZ(\omega)] = 0 \\ &\mathbb{E}[|dZ(\omega)|^2] = S(\omega)d\omega \\ &\mathbb{E}[dZ(\omega_1)dZ(\omega_2)dZ^*(\omega_3)] = \delta(\omega_1 + \omega_2 - \omega_3)B(\omega_1,\omega_2)d\omega_1 d\omega_2 \end{aligned} \tag{13}$$

Notice that the measure $d\mu(\omega) = S(\omega)d\omega$ in the second-order condition and that the third-order condition introduces an associated stationary bispectrum $B(\omega_1,\omega_2)$. Analogous to Eq. (9), we define the evolutionary bispectrum as

$$\begin{aligned} B(t,\omega_1,\omega_2) &= A(t,\omega_1)A(t,\omega_2)A(t,\omega_1+\omega_2)\mathbb{E}[dZ(\omega_1)dZ(\omega_2)dZ^*(\omega_1+\omega_2)] \\ B(t,\omega_1,\omega_2) &= A(t,\omega_1)A(t,\omega_2)A(t,\omega_1+\omega_2)B(\omega_1,\omega_2) \end{aligned} \tag{14}$$

such that it represents the distribution of the skewness over the space of frequency pairs at any given time, analogous to Priestley's [16] evolutionary spectrum distributing the variance over the frequency domain at any given time. This is shown in more detail in Appendix C.

Next, consider that the orthogonal increments $dZ(\omega)$ can be divided into their real and complex components as

$$\begin{aligned} dU(\omega) &= \mathrm{Re}[dZ(\omega)], \\ dV(\omega) &= -\mathrm{Im}[dZ(\omega)] \end{aligned} \tag{15}$$

where the individual increments $dU(\omega)$ and $dV(\omega)$ satisfy

$$\mathbb{E}[dU(\omega)] = \mathbb{E}[dV(\omega)] = 0 \tag{16}$$

Similarly, the modulating function $A(t,\omega)$ can be divided into real and complex components as

$$A(t,\omega) = \alpha(t,\omega) + \imath\beta(t,\omega) \tag{17}$$

Applying these relations, the spectral representation in (7) can be rewritten as

$$X(t) = \int_{-\infty}^{\infty} [\alpha(t,\omega) + \imath\beta(t,\omega)][\cos(\omega t) + \imath \sin(\omega t)][dU(\omega) - \imath dV(\omega)] \tag{18}$$

and is equivalently represented as

$$X(t) = \int_{-\infty}^{\infty} \cos(\omega t) dU_t(\omega) - \sin(\omega t) dV_t(\omega) \tag{19}$$

where

$$dU_t(\omega) = \alpha(t,\omega) dU(\omega) + \beta(t,\omega) dV(\omega) \tag{20}$$

$$dV_t(\omega) = \beta(t,\omega) dU(\omega) - \alpha(t,\omega) dV(\omega) \tag{21}$$

are modulated orthogonal increments satisfying the following properties (see Appendix A)

$$\begin{aligned} &\mathbb{E}[dU_t(\omega)] = \mathbb{E}[dV_t(\omega)] = 0 \\ &\mathbb{E}[dU_t^2(\omega)] = \mathbb{E}[dV_t^2(\omega)] = 2S(\omega,t)d\omega \\ &\mathbb{E}[dU_t(\omega_1)dU_t(\omega_2)dU_t(\omega_1+\omega_2)] = \mathbb{E}[dV_t(\omega_1)dV_t(\omega_2)dV_t(\omega_1+\omega_2)] = \\ &= 2B(t,\omega_1,\omega_2)d\omega_1 d\omega_2 \end{aligned} \tag{22}$$

### 3.2. Simulation of 3rd-order non-stationary stochastic processes

To enable simulation, we propose the following modulated orthogonal increments that satisfy the required properties

$$\begin{aligned} dU_t(\omega_k) = {} & [2S_p(t,\omega_k)\Delta\omega]^{\frac{1}{2}} \cos(\phi_k) \\ & + \sum_{i+j=k}^{i\geq j\geq 0} [2S(t,\omega_k)\Delta\omega]^{\frac{1}{2}} |b_p(t,\omega_i,\omega_j)| \cos(\phi_i + \phi_j + \beta(t,\omega_i,\omega_j)) \end{aligned} \tag{23}$$

$$\begin{aligned} dV_t(\omega_k) = {} & [2S_p(t,\omega_k)\Delta\omega]^{\frac{1}{2}} \sin(\phi_k) \\ & + \sum_{i+j=k}^{i\geq j\geq 0} [2S(t,\omega_k)\Delta\omega]^{\frac{1}{2}} |b_p(t,\omega_i,\omega_j)| \sin(\phi_i + \phi_j + \beta(t,\omega_i,\omega_j)) \end{aligned} \tag{24}$$

where $S(t,\omega)$ is the evolutionary power spectrum, $S_p(t,\omega)$ is the pure component of the evolutionary power spectrum defined as

$$S_p(t,\omega_k) = S(t,\omega_k)(1 - \sum_{i+j=k}^{i\geq j\geq 0} b_p^2(t,\omega_i,\omega_j)) \tag{25}$$

and $b_p(t,\omega_i,\omega_j)$ is the partial evolutionary bicoherence given by

$$b_p^2(t,\omega_i,\omega_j) = \frac{|B(t,\omega_i,\omega_j)|^2 \Delta\omega}{S_p(t,\omega_i)S_p(t,\omega_j)S(t,\omega_i+\omega_j)} \tag{26}$$

where $B(t,\omega_1,\omega_2)$ is the evolutionary bispectrum. Note that the pure evolutionary power spectrum and the evolutionary bicoherence result from a direct extension of their stationary counterparts introduced in [14].

Using the above definitions for the modulated orthogonal increments, the stochastic process in Eq. (19) process can be expanded as

$$\begin{aligned} X(t) = {} & 2\sum_{k=-\infty}^{\infty} \sqrt{S_p(t,\omega_k)\Delta\omega} \cos(\omega_k t + \phi_k) \\ & + 2\sum_{k=0}^{N-1} \sum_{i+j=k}^{i\geq j\geq 0} \sqrt{S(t,\omega_k)\Delta\omega} |b_p(t,\omega_i,\omega_j)| \cos(\omega_k t + \phi_i + \phi_i + \beta(t,\omega_i,\omega_j)) \end{aligned} \tag{27}$$

where $\beta(t,\omega_i,\omega_j)$ is the evolutionary biphase given by

$$\beta(t,\omega_i,\omega_j) = \arctan\left(\frac{\mathrm{Im}\{B(t,\omega_1,\omega_2)\}}{\mathrm{Re}\{B(t,\omega_1,\omega_2)\}}\right) \tag{28}$$

where $\mathrm{Im}\{\cdot\}$ represents the imaginary part, $\mathrm{Re}\{\cdot\}$ represents the real part and

$$\begin{aligned} &\Delta\omega = \frac{\omega_u}{N} \\ &\omega_k = k\Delta\omega \;\; k = 0,1,2,\ldots,N-1 \end{aligned} \tag{29}$$

and $\omega_u$ is the upper cutoff frequency beyond which the evolutionary power spectral density function $S(t,\omega)$ may be assumed to be zero. Finally, it is assumed that $S(t,\omega_0) = 0$.

It is shown in Appendix B that the above non-stationary process satisfies the correct ensemble statistical properties up to third-order.

The infinite series representation in Eq. (27) can be truncated with to include $N$ terms for simulation purposes as

$$\begin{aligned} X(t) &= 2\sum_{k=0}^{N-1}\sqrt{S_p(t,\omega_k)\Delta\omega}\cos(\omega_k t+\phi_k) \\ &+ 2\sum_{k=0}^{N-1}\sum_{i+j=k}^{i\geq j\geq 0}\sqrt{S(t,\omega_k)\Delta\omega}|b_p(t,\omega_i,\omega_j)|\cos(\omega_k t+\phi_i+\phi_i+\beta(t,\omega_i,\omega_j)) \end{aligned} \tag{30}$$

Finally, after some rearrangement, the simulation formula can be expressed as

$$\begin{aligned} X(t) = 2\sum_{k=0}^{N-1}\sqrt{S(t,\omega_k)\Delta\omega}\Bigg[&\sqrt{(1-\sum_{i+j=k}^{i\geq j\geq 0}b_p^2(t,\omega_i,\omega_j))}\cos(\omega_k t+\phi_k) \\ &+\sum_{i+j=k}^{i\geq j\geq 0}|b_p(t,\omega_i,\omega_j)|\cos(\omega_k t+\phi_i+\phi_i+\beta(t,\omega_i,\omega_i))\Bigg] \end{aligned} \tag{31}$$

The computational complexity of the simulation formula is of the order $O(MN^2)$, where $M$ is the number of time discretizations, which leads to high computational expense for simulations in this form. Given the computational expense, we propose an alternative formulation that leverages the proper orthogonal decomposition (POD) next.

## 4. POD based implementation of 3-order spectral representation method

Li and Kareem [19] first proposed the use of the POD technique to enable the use of the Fast Fourier Transform (FFT) for the simulation of non-stationary random processes. POD for the 2nd Spectral Representation Method involves the decomposition of $\sqrt{S(t,\omega)}$ in Eq. (10) into a sum of separable frequency and time functions as

$$\sqrt{S(t,\omega)} = \sum_{q=1}^{N_q} a_q(t)\Phi_q(\omega) \tag{32}$$

where $\Phi_q(\omega)$ are orthogonal functions and $a_q(t)$ are time-dependent principal coordinate vectors calculated by $a_q(t) = \int_\omega \sqrt{S(t,\omega)}\,\Phi_q(\omega)$. After decomposing the evolutionary power spectrum into the set of time and frequency functions $a_q(t), \Phi_q(\omega)$, the simulation formula in Eq. (10) can be expressed as

$$X(t) = \sum_{q=1}^{N_q} 2a_q(t)\sum_{n=0}^{N-1}\Phi_q(\omega_n)\sqrt{\Delta\omega}\cos(\omega_n t+\phi_n^q) \tag{33}$$

This is equivalent to a sum of modulated stationary random processes. Since an individual stationary random process can be simulated using FFT, the non-stationary process can be simulated as a sum of processes simulated using FFT.

In the remainder of the section, we develop the POD-based implementation for simulation of non-stationary processes by 3rd-order Spectral Representation Method.

Recall the simulation formula in Eq. (27). Let us apply the Tucker decomposition [30] on the second term as

$$\frac{|B(t,\omega_1,\omega_2)|}{\sqrt{S_p(t,\omega_1)S_p(t,\omega_2)}} = \mathcal{T}\times_1 U^{(1)}\times_2 U^{(2)}\times_3 U^{(3)} \tag{34}$$

where $\mathcal{T}$ is the core tensor and $U^{(1)}, U^{(2)}, U^{(3)}$ are unitary matrices. A set of orthogonal functions $\Phi_q(\omega)$ is chosen to be the columns of the matrix $U^{(3)}$. From the set of basis functions $\Phi_q(\omega)$, we can form a second-order basis as

$$\theta_{rs}(\omega_1,\omega_2) = \Phi_r(\omega_1)\Phi_s(\omega_2) \tag{35}$$

This allow us to decouple the time and frequency components in the interactive component of the simulation formula, $\frac{B(t,\omega_1,\omega_2)}{\sqrt{S_p(t,\omega_1)S_p(t,\omega_2)}}$, which depend on frequency pairs. The corresponding set of projected bispectrum amplitude functions $b_{rs}(t)$ can be computed by

$$\begin{aligned} b_{rs}(t) &= \int_{\omega_1,\omega_2}\theta_{rs}(\omega_1,\omega_2)\frac{B(t,\omega_1,\omega_2)}{\sqrt{S_p(t,\omega_1)S_p(t,\omega_2)}} \\ &= \int_{\omega_1,\omega_2}\Phi_r(\omega_1)\Phi_s(\omega_2)\frac{B(t,\omega_1,\omega_2)}{\sqrt{S_p(t,\omega_1)S_p(t,\omega_2)}} \end{aligned} \tag{36}$$

where the reconstruction can be expressed as

$$\frac{B(t,\omega_1,\omega_2)}{\sqrt{S_p(t,\omega_1)S_p(t,\omega_2)}} \approx \sum_{r,s} b_{rs}(t)\theta_{rs}(\omega_1,\omega_2). \tag{37}$$

This represents the higher-order analogue to Eq. (32) – i.e. the separation of the bispectrum into orthogonal frequency functions and corresponding time-dependent modulating functions — and further allows the pure component of the power spectrum to be decomposed as

$$\begin{aligned}\sqrt{S_p(t,\omega)} &\approx \sum_{q=1} a_q(t)\Phi_q(\omega)\\ a_q(t) &= \int_\omega \sqrt{S_p(t,\omega)}\Phi_q(\omega)\end{aligned} \tag{38}$$

Note that the projected amplitude function $b_{rs}(t)$ function can be complex-valued since the non-stationary Bispectrum $B(t,\omega_i,\omega_j)$ can be complex-valued. Each of these functions can be expressed with a set of biphase angles $\gamma_{rs}(t)$ as

$$b_{rs}(t) = |b_{rs}(t)|e^{i\gamma_{rs}(t)} \tag{39}$$

Substituting the functions $\Phi_q(\omega), a_q(t), b_{rs}(t)$ into the simulation formula yields

$$\begin{aligned}X(t) = 2\sum_{k=0}^{N-1}\Bigg[&\sum_{q=1}^{N_q} a_q(t)\Phi_q(\omega_k)\sqrt{\Delta\omega}\cos(\omega_k t-\phi_{kq})\\ &+\sum_{i+j=k}^{i\geq j\geq 0}\sum_{r=1}^{N_q}\sum_{s=1}^{N_q}|b_{rs}(t)|\theta_{rs}(\omega_i,\omega_j)\Delta\omega\cos(\omega_k t-\phi_{ri}-\phi_{sj}+\gamma_{rs}(t))\Bigg]\end{aligned} \tag{40}$$

which can be further simplified to

$$\begin{aligned}X(t) &= 2\sum_{k=0}^{N-1}\sum_{r=1}^{N_q}\Bigg[a_r(t)\Phi_r(\omega_k)\sqrt{\Delta\omega}\cos(\omega_k t-\phi_{kr})\\ &\quad+\sum_{i+j=k}^{i\geq j\geq 0}\sum_{s=1}^{N_q}|b_{rs}(t)|\theta_{rs}(\omega_i,\omega_j)\Delta\omega\cos(\omega_k t-\phi_{ri}-\phi_{sj}+\gamma_{rs}(t))\Bigg]\\ X(t) &= 2\sum_{r=1}^{N_q}x_r(t)\end{aligned} \tag{41}$$

where

$$\begin{aligned}x_r(t) = \sum_{k=0}^{N-1}\Bigg[&a_r(t)\Phi_r(\omega_k)\sqrt{\Delta\omega}\cos(\omega_k t-\phi_{kr})\\ &+\sum_{i+j=k}^{i\geq j\geq 0}\sum_{s=1}^{N_q}|b_{rs}(t)|\theta_{rs}(\omega_i,\omega_j)\Delta\omega\cos(\omega_k t-\phi_{ri}-\phi_{sj}+\gamma_{rs}(t))\Bigg]\end{aligned} \tag{42}$$

That is, the third-order non-stationary process can be simulated as the sum of modulated third-order stationary processes, $x_r(t)$. We observe from [15] that $x_q(t)$ can be simulated using FFT, and therefore the full non-stationary third-order stochastic process $X(t)$ can also be simulated using FFT.

The processes simulated by the POD method satisfies the required second and third properties as shown in Appendices D and E. Finally, the number of components $N_q$ in the expansion from Eq. (34) should then be chosen such that the approximation Eq. (37) is sufficiently accurate. As we show in the numerical examples that follow, this number $N_q$ is often small. The computational complexity of the POD based implementation is of the order

$$O(N_q^2N^2 + N_q^2M\log N), \tag{43}$$

which provides considerable time savings over the original simulation equation, which again is $O(MN^2)$, as long as $N_q^2 \ll M$.

## 5. Numerical examples

In this section we present two examples for the simulation of non-stationary stochastic processes by 3rd-order Spectral Representation Method. The first example involves the simulation of a stochastic process with separable time and frequency components which provides intuition to understand the POD based implementation. The second example considers the simulation of a fully non-stationary stochastic ground motion process using the Clough–Penzien power spectrum, which highlights the practical application of the simulation formula.

### 5.1. Example 1: Non-stationary process with separable time and frequency contributions

Let $f_s(t)$ represent a stationary stochastic process simulated using the 3rd-order Spectral Representation Method [15] from power spectrum $S(\omega)$ and bispectrum $B(\omega_1,\omega_2)$. Consider the evolutionary power spectral density takes the amplitude modulated form

$$S(t,\omega) = M^2(t)S(\omega) \tag{44}$$

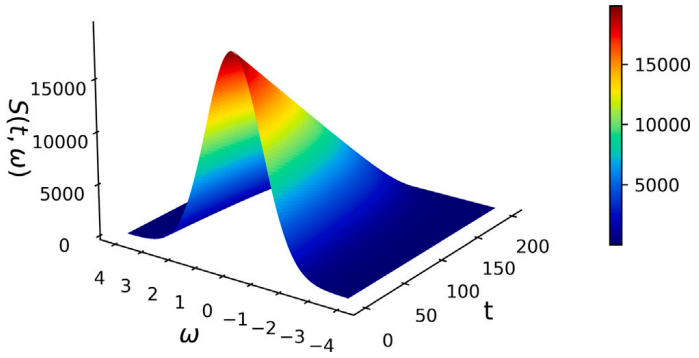


**Fig. 1.** Example 1: Time–frequency separable evolutionary power spectral density.

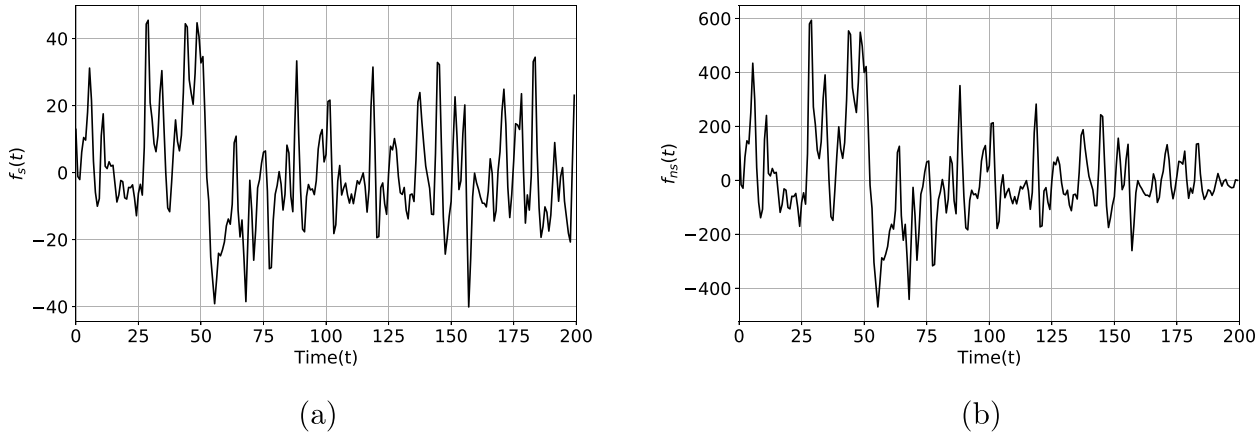


**Fig. 2.** Example 1: Sample functions of (a) the stationary process $f_s(t)$ and (b) the amplitude modulated non-stationary processes $f_{ns}(t)$.

and the evolutionary bispectrum takes a similar amplitude modulated form given by

$$B(t,\omega_1,\omega_2) = M(t)^3 B(\omega_1,\omega_2). \tag{45}$$

The resulting non-stationary process then takes the form

$$f_{ns}(t) = M(t) f_s(t) \tag{46}$$

The function $M(t)$ is simply a time-dependent modulating function which modifies the amplitude (but not the frequency content) of the stationary process to introduce non-stationarity.

Consider the specific evolutionary power spectrum of this form given by

$$S(t,\omega) = 100(200-t)e^{-\frac{1}{2}\omega^2} \tag{47}$$

where $M(t) = \sqrt{200-t}$ and $S(\omega) = 100e^{-\frac{1}{2}\omega^2}$ which is plotted in Fig. 1.

The corresponding evolutionary bispectrum takes the form

$$B(t,\omega_1,\omega_2) = \frac{2000}{3\sqrt{3(\omega_1+\omega_2)}}(200-t)^{\frac{3}{2}} e^{-\frac{1}{2}(\omega_1^2+\omega_2^2+\omega_1\omega_2)}. \tag{48}$$

Since $M(t) = \sqrt{200-t}$, we can see that

$$B(\omega_1,\omega_2) = \frac{2000}{3\sqrt{3(\omega_1+\omega_2)}} e^{-\frac{1}{2}(\omega_1^2+\omega_2^2+\omega_1\omega_2)} \tag{49}$$

The parameters used in the simulations are as follows

$$T = 200\text{s} \quad \omega_0 = 4.02 \text{ rad/s} \quad M = 256 \quad N = 128 \tag{50}$$

Sample functions of the stationary process, $f_s(t)$, and the non-stationary process, $f_{ns}(t)$, are plotted in Fig. 2.

Fig. 3 shows the time-evolution of the second moment, third moment, and skewness of the process computed from 10,000 sample non-stationary processes along with theoretical values derived from the evolutionary spectra. We can see that the properties of the simulated non-stationary processes closely match the theoretical values.

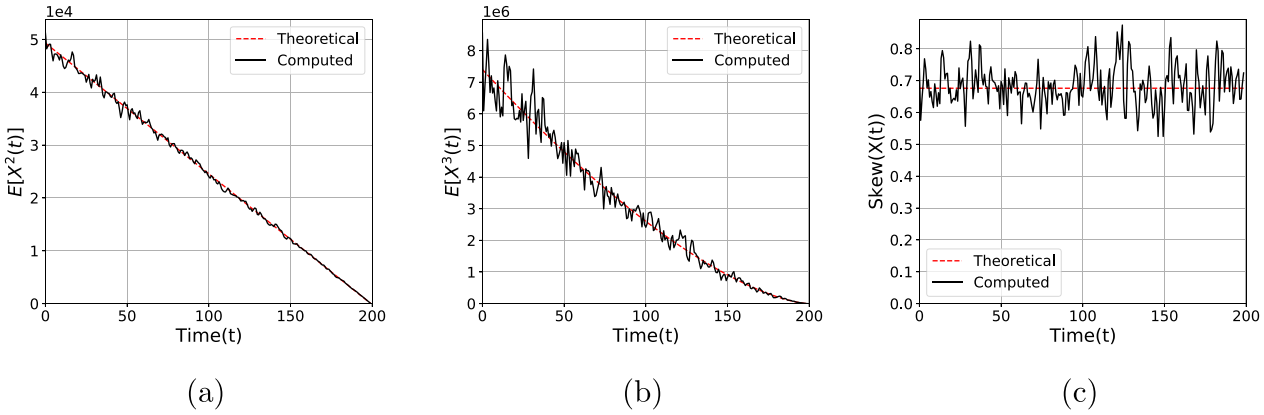


**Fig. 3.** Example 1: Time evolution of (a) the second moment, (b) the third moment, and (c) the skewness for the separable non-stationary stochastic process.

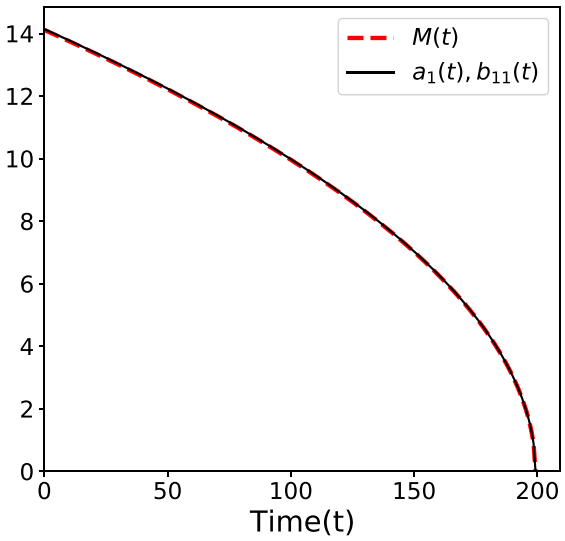


**Fig. 4.** Example 1: Modulating Function $M(t)$ and the first time-dependent amplitude functions $a_1(t), b_{11}(t)$ from the POD for the separable evolutionary power spectrum.

Proper Orthogonal Decomposition of the evolutionary power spectrum reveals that the first component in the pure component of the expansion $a_1(t)$ and the interactive component of the expansion $b_{11}(t)$ are both equal to the modulating function $M(t)$ as seen in Fig. 4. This demonstrates that the POD can successfully decompose a separable evolutionary power spectra with only a single orthogonal component. This further illustrates the interpretation that the POD based implementation is akin to finding a series of modulating functions and underlying stationary spectra.

### 5.2. Non-stationary seismic ground motion

Next, we consider the simulation of a non-stationary stochastic ground motion process using the Kanai–Tajimi evolutionary power spectrum with Clough–Penzien correction [31], which contains both frequency and amplitude modulation. The equation for the Kanai–Tajimi evolutionary spectrum is given by

$$S_{kt}(t,\omega) = \frac{1 + 4\zeta_g^2\left(\frac{\omega}{\omega_g}\right)^2}{\left[1 - \left(\frac{\omega}{\omega_g}\right)^2\right]^2 + 4\zeta_g^2\left(\frac{\omega}{\omega_g}\right)^2}, \tag{51}$$

and the Clough–Penzien correction factor is defined as

$$\gamma_{cp}(t,\omega) = \frac{\left(\frac{\omega}{\omega_f}\right)^4}{\left[1 - \left(\frac{\omega}{\omega_f}\right)^2\right]^2 + 4\zeta_f^2\left(\frac{\omega}{\omega_f}\right)^2} \tag{52}$$

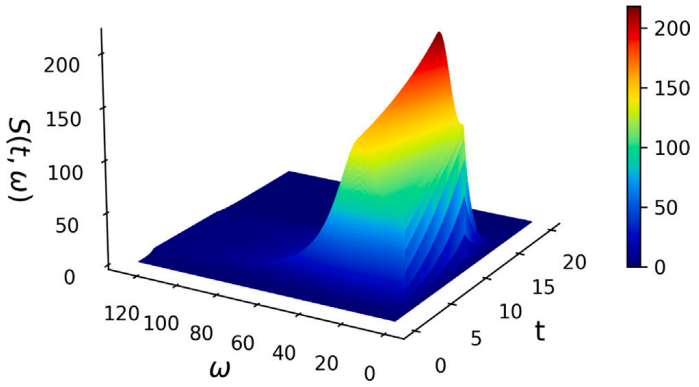


**Fig. 5.** Example 2: Clough–Penzien Evolutionary Spectrum.

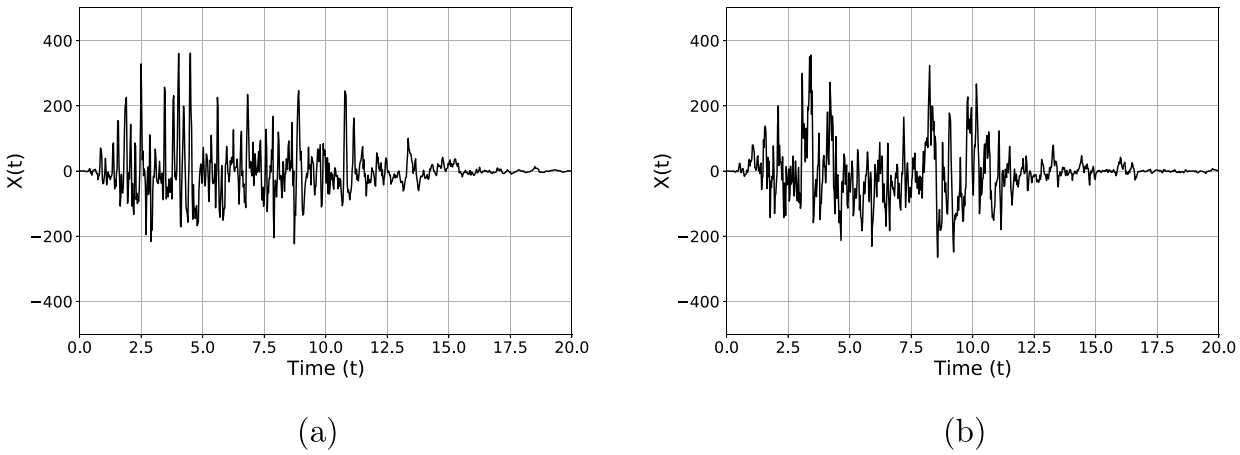


**Fig. 6.** Example 2: Representative sample functions of the third-order non-stationary stochastic ground motion process simulated using (a) the direct sum of cosines and (b) the POD implementation.

where the time-dependent, non-stationary parameters are defined as

$$\begin{aligned} \omega_g &= 30 - 1.25t \\ \omega_f &= 0.1\omega_g \\ \zeta_g &= 0.5 + 0.005t \\ \zeta_f &= 0.1\zeta_g \end{aligned} \tag{53}$$

such that $\omega_g$, $\zeta_g$ are the characteristic frequency and damping of the ground and $\omega_f$, $\zeta_f$ are the filtering parameters of the Clough–Penzien correction. The resulting Clough–Penzien evolutionary power spectrum is given by

$$S_{cp}(t,\omega) = S_{kt}(t,\omega)\gamma_{cp}(t,\omega) \tag{54}$$

and is plotted in Fig. 5. We define the associated bispectrum of the non-stationary process as

$$B(t,\omega_i,\omega_j) = \frac{2\sqrt{S_{cp}(t,\omega_i)S_{cp}(t,\omega_j)S_{cp}(t,\omega_i+\omega_j)}}{3\sqrt{3(\omega_i+\omega_j)}} \tag{55}$$

The non-stationary process is simulated using both the direct sum of cosines and the POD-based implementation. The parameters of the simulation are given by

$$T = 20 \quad \omega_0 = 125.66 \text{ rad/sec} \quad M = 800 \quad N = 400 \quad n_q = 10 \tag{56}$$

Sample function plots for each implementation are shown in Fig. 6, demonstrating that both methods are capable of simulating the random process.

Sample statistics of the simulated process at three different time instants from 10,000 simulations using both the sum of cosines and POD implementation with increasing number of POD components are shown in Figs. 7, 8. The dotted lines in these plots represents the theoretical values, while the solid lines represent the simulation results. We can see that the statistics converge very

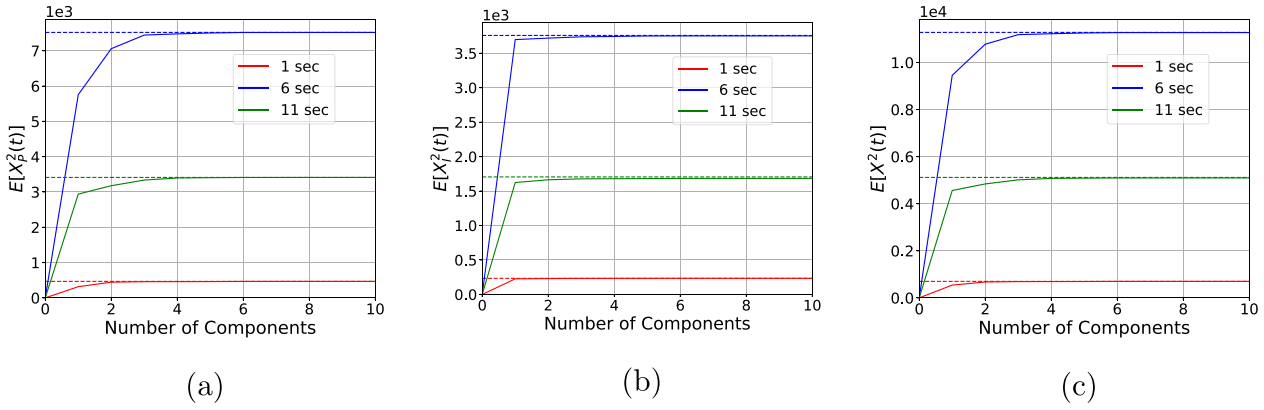


**Fig. 7.** Example 2: Convergence of (a) the pure component of the second moment, (b) the interactive component of the second moment, and (c) the total second moment at different time instances with increasing number of POD components.

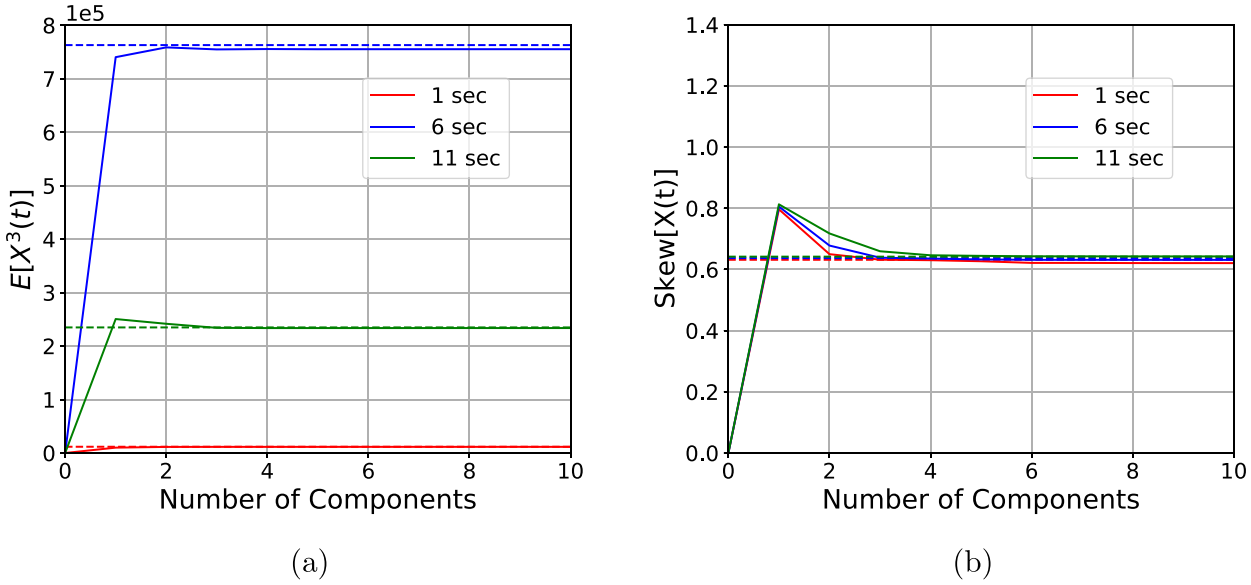


**Fig. 8.** Example 2: Convergence of (a) the third moment, and (b) the skewness at different time instances with increasing number of POD components.

rapidly with only 4 POD components. We further plot the time-varying second and third moments of the simulated process, estimated from 100,000 samples, using the first 4 POD modes in Fig. 9 along with their theoretical values.

Here, we can see that the statistical properties of the process match the their theoretical moments with high accuracy throughout the time duration of the process. To demonstrate the accuracy in representing higher-order correlations, slices across the $t_1$ axis of the three point correlation function $R_3(t_1, t_2, t_3)$ at $t_1 = 10$ s are shown for the sum of cosines implementation and POD implementation along with their theoretical values in 10. We can see that the numerical results from the sum of cosines formula agree with the theoretical results closely while the three point correlation function of the samples from the POD implementation have some very slight discrepancies. This could be reduced by including more components in the POD expansion ($n_q > 4$) or increasing the number of samples to generate the results.

Next, we compare the computation time for simulation of non-stationary processes by the $2^{nd}$-order and $3^{rd}$-order Spectral Representation Method using both the standard sum of cosines approach and the POD methods for increasing number of samples. Results are shown in Tables 1 and 2 for the $2^{nd}$-order and $3^{rd}$-order SRM, respectively.

The tables show total CPU time for both the sum of cosines approach and the POD based implementation, where times for POD based implementation are broken down into three components: total CPU time, CPU time for the POD of the evolutionary power spectrum, and CPU time for simulation of the stationary samples using FFT. We can see that the time for the POD remains constant, while the FFT simulation scales with the number of simulations. Hence, the computation time will scale with sample size and with $N_q$ (i.e. the number of FFTs required for a single simulation). More specifically, simulation time is proportional to the square of $N_q$ in the POD method (see Eq. (43)), so choosing fewer components helps drastically reduce the simulation time. The tables further show that for the given $M$ and $N$, i.e. the given number of time and frequency intervals, using the POD based implementation is

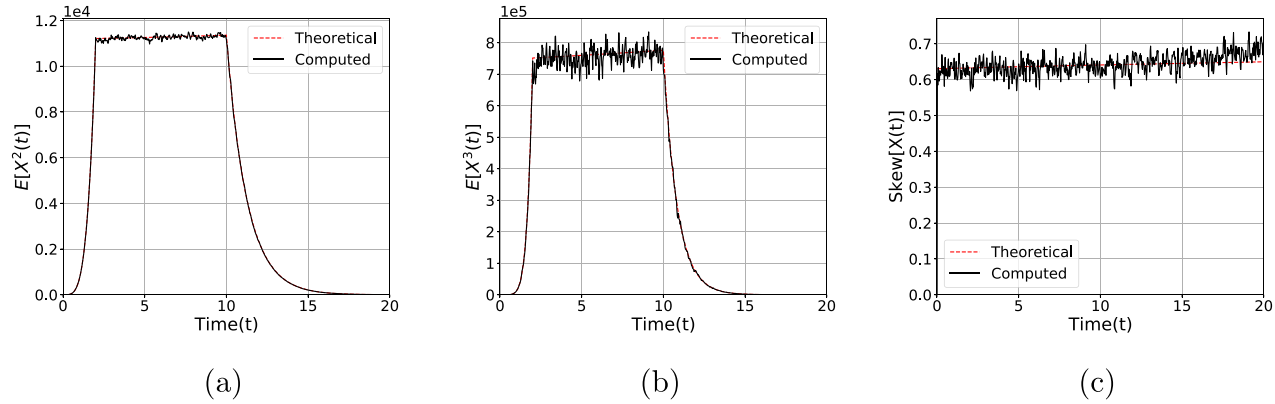


**Fig. 9.** Example 2: Evolution of (a) second-order moment(variance), (b) third-order moment and (c) skewness with time.

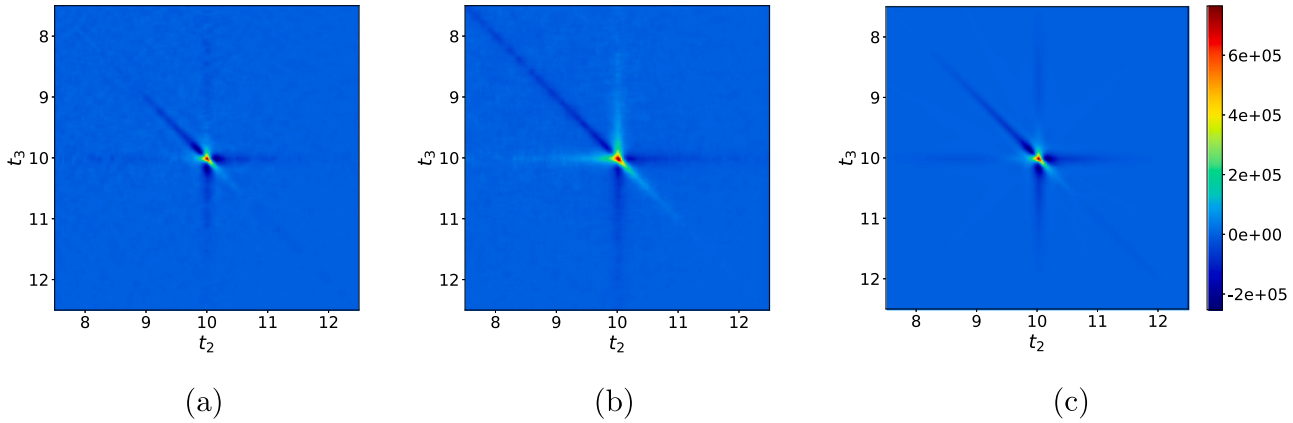


**Fig. 10.** Example 2: The slice of the three point correlation function $R_3(t_1, t_2, t_3)$ at $t_1 = 10$ for (a) Sum of cosines implementation (b) POD implementation and (c) Theoretical.

**Table 1**
Comparison of computation time for the sum of cosines formula and the POD method for simulating 2nd-order non-stationary stochastic ground motion processes.

| Number of samples | Time (s) | | | |
|---|---|---|---|---|
| | Sum of cosines | POD | | |
| | | Total | Decomposition | Simulation |
| 1 | 3.0971 | 0.7885 | 0.7864 | 0.0021 |
| 10 | 3.4194 | 0.7705 | 0.7614 | 0.0091 |
| 100 | 5.1791 | 0.8472 | 0.7590 | 0.0882 |
| 1000 | 29.0474 | 1.7306 | 0.7603 | 0.9703 |
| 10000 | 250.0017 | 16.5228 | 0.7630 | 15.7598 |
| 100000 | 2738.2145 | 137.4785 | 0.7633 | 136.7152 |

**Table 2**
Comparison of the computation time for the sum of cosines formula and the POD method for simulating 3rd-order non-stationary stochastic ground motion processes.

| Number of samples | Time (s) | | | |
|---|---|---|---|---|
| | Sum of cosines | POD | | |
| | | Total | Decomposition | Simulation |
| 1 | 435.1617 | 36.7289 | 22.9394 | 13.7895 |
| 10 | 480.0146 | 39.0056 | 23.4440 | 15.5616 |
| 100 | 659.3620 | 39.3217 | 23.3529 | 15.9688 |
| 1000 | 3322.8135 | 71.7228 | 23.5590 | 48.1638 |

always computationally beneficial for both 2nd and 3rd-order processes, even when simulating only a single sample function. Note that, in Table 2, we do not simulate more than 1000 realizations because the sum of cosines implementation become intractable.

## 6. Conclusion

In this paper, the 3rd-order Spectral Representation Method has been extended for the simulation of non-stationary stochastic processes. First, the standard sum of cosines form was derived. This conventional implementation is computationally prohibitive. To alleviate the computational burden, a Proper Orthogonal Decomposition (POD) based implementation was presented, which enables the use of Fast Fourier Transform to significant speed up the simulations. Two example processes are simulated to highlight the advantages of the proposed method. The first example considers a time–frequency separable process, where we show that the POD implementation correctly separates the components for simulation. The second example considers an inseparable ground motion process, demonstrating convergence of the POD implementation in the statistical response using only a small number of components. The second example further explores the computational gains afforded by the POD implementation and demonstrates that the POD implementation can be orders of magnitude more efficient and enable the simulation of processes that are infeasible to simulate with the standard sum of cosines implementation.

## Declaration of competing interest

The authors declare that they have no known competing financial interests or personal relationships that could have appeared to influence the work reported in this paper.

## Acknowledgment

This work has been supported by the National Science Foundation under award number 1652044.

## Appendix A. Spectral properties of the modulated orthogonal increments

Herein, we demonstrate the orthogonality properties of the modulated orthogonal increments in the third-order non-stationary spectral representation given in Eqs. (20) and (21).

Let us begin with the first-order orthogonality condition where it follows that

$$\mathbb{E}[dU_t(\omega)] = \alpha(t,\omega)\mathbb{E}[dU(\omega)] + \beta(t,\omega)\mathbb{E}[dV(\omega)] = 0 \tag{A.1}$$

$$\mathbb{E}[dV_t(\omega)] = \beta(t,\omega)\mathbb{E}[dU(\omega)] - \alpha(t,\omega)\mathbb{E}[dV(\omega)] = 0 \tag{A.2}$$

due to the fact that $dU(\omega) = dV(\omega) = 0$

Next, consider the second-order orthogonality condition where

$$\begin{aligned}\mathbb{E}[dU_t^2(\omega)] &= \alpha^2(t,\omega)\mathbb{E}[dU^2(\omega)] + \beta^2(t,\omega)\mathbb{E}[dV^2(\omega)] \\ &\quad + 2\alpha(t,\omega)\beta(t,\omega)\mathbb{E}[dU(\omega)dV(\omega)] \\ &= 2(\alpha^2(t,\omega) + \beta^2(t,\omega))S(\omega)d\omega \\ &= 2|A(t,\omega)|^2 S(\omega)d\omega \\ &= 2S(t,\omega)d\omega\end{aligned} \tag{A.3}$$

$$\begin{aligned}\mathbb{E}[dV_t^2(\omega)] &= \beta^2(t,\omega)\mathbb{E}[dU^2(\omega)] + \alpha^2(t,\omega)\mathbb{E}[dV^2(\omega)] \\ &\quad - 2\alpha(t,\omega)\beta(t,\omega)\mathbb{E}[dU(\omega)dV(\omega)] \\ &= 2(\alpha^2(t,\omega) + \beta^2(t,\omega))S(\omega)d\omega \\ &= 2|A(t,\omega)|^2 S(\omega)d\omega \\ &= 2S(t,\omega)d\omega\end{aligned} \tag{A.4}$$

Finally, the third-order orthogonality condition yields

$$
\begin{aligned}
&\mathbb{E}[dU_t(\omega_1)dU_t(\omega_2)dU_t(\omega_1+\omega_2)]\\
&=\alpha(t,\omega_1)\alpha(t,\omega_2)\alpha(t,\omega_1+\omega_2)\mathbb{E}[dU(\omega_1)dU(\omega_2)dU(\omega_1+\omega_2)]\\
&+\alpha(t,\omega_1)\alpha(t,\omega_2)\beta(t,\omega_1+\omega_2)\mathbb{E}[dU(\omega_1)dU(\omega_2)dV(\omega_1+\omega_2)]\\
&+\alpha(t,\omega_1)\beta(t,\omega_2)\alpha(t,\omega_1+\omega_2)\mathbb{E}[dU(\omega_1)dV(\omega_2)dU(\omega_1+\omega_2)]\\
&+\beta(t,\omega_1)\alpha(t,\omega_2)\alpha(t,\omega_1+\omega_2)\mathbb{E}[dV(\omega_1)dU(\omega_2)dU(\omega_1+\omega_2)]\\
&+\alpha(t,\omega_1)\beta(t,\omega_2)\beta(t,\omega_1+\omega_2)\mathbb{E}[dU(\omega_1)dV(\omega_2)dV(\omega_1+\omega_2)]\\
&+\beta(t,\omega_1)\alpha(t,\omega_2)\beta(t,\omega_1+\omega_2)\mathbb{E}[dV(\omega_1)dU(\omega_2)dV(\omega_1+\omega_2)]\\
&+\beta(t,\omega_1)\beta(t,\omega_2)\alpha(t,\omega_1+\omega_2)\mathbb{E}[dV(\omega_1)dV(\omega_2)dU(\omega_1+\omega_2)]\\
&+\beta(t,\omega_1)\beta(t,\omega_2)\beta(t,\omega_1+\omega_2)\mathbb{E}[dV(\omega_1)dV(\omega_2)dV(\omega_1+\omega_2)]\\
&=2\alpha(t,\omega_1)\alpha(t,\omega_2)\alpha(t,\omega_1+\omega_2)\mathbb{R}B(\omega_1,\omega_2)d\omega_1 d\omega_2\\
&-2\alpha(t,\omega_1)\alpha(t,\omega_2)\beta(t,\omega_1+\omega_2)\mathbb{I}B(\omega_1,\omega_2)d\omega_1 d\omega_2\\
&+2\alpha(t,\omega_1)\beta(t,\omega_2)\alpha(t,\omega_1+\omega_2)\mathbb{I}B(\omega_1,\omega_2)d\omega_1 d\omega_2\\
&+2\beta(t,\omega_1)\alpha(t,\omega_2)\alpha(t,\omega_1+\omega_2)\mathbb{I}B(\omega_1,\omega_2)d\omega_1 d\omega_2\\
&+2\alpha(t,\omega_1)\beta(t,\omega_2)\beta(t,\omega_1+\omega_2)\mathbb{R}B(\omega_1,\omega_2)d\omega_1 d\omega_2\\
&+2\beta(t,\omega_1)\alpha(t,\omega_2)\beta(t,\omega_1+\omega_2)\mathbb{R}B(\omega_1,\omega_2)d\omega_1 d\omega_2\\
&-2\beta(t,\omega_1)\beta(t,\omega_2)\alpha(t,\omega_1+\omega_2)\mathbb{R}B(\omega_1,\omega_2)d\omega_1 d\omega_2\\
&+2\beta(t,\omega_1)\beta(t,\omega_2)\beta(t,\omega_1+\omega_2)\mathbb{I}B(\omega_1,\omega_2)d\omega_1 d\omega_2\\
&=2A^*(t,\omega_1)A^*(t,\omega_2)A(t,\omega_1+\omega_2)\mathbb{E}[dZ^*(\omega_1)dZ^*(\omega_2)dZ^*(\omega_1+\omega_2)]\\
&=2B(t,\omega_1,\omega_2)d\omega_1 d\omega_2
\end{aligned}
\tag{A.5}
$$

$$
\begin{aligned}
&\mathbb{E}[dV_t(\omega_1)dV_t(\omega_2)dV_t(\omega_1+\omega_2)]\\
&=\beta(t,\omega_1)\beta(t,\omega_2)\beta(t,\omega_1+\omega_2)\mathbb{E}[dU(\omega_1)dU(\omega_2)dU(\omega_1+\omega_2)]\\
&-\beta(t,\omega_1)\beta(t,\omega_2)\alpha(t,\omega_1+\omega_2)\mathbb{E}[dU(\omega_1)dU(\omega_2)dV(\omega_1+\omega_2)]\\
&-\beta(t,\omega_1)\alpha(t,\omega_2)\beta(t,\omega_1+\omega_2)\mathbb{E}[dU(\omega_1)dV(\omega_2)dU(\omega_1+\omega_2)]\\
&-\alpha(t,\omega_1)\beta(t,\omega_2)\beta(t,\omega_1+\omega_2)\mathbb{E}[dV(\omega_1)dU(\omega_2)dU(\omega_1+\omega_2)]\\
&+\beta(t,\omega_1)\alpha(t,\omega_2)\alpha(t,\omega_1+\omega_2)\mathbb{E}[dU(\omega_1)dV(\omega_2)dV(\omega_1+\omega_2)]\\
&+\alpha(t,\omega_1)\beta(t,\omega_2)\alpha(t,\omega_1+\omega_2)\mathbb{E}[dV(\omega_1)dU(\omega_2)dV(\omega_1+\omega_2)]\\
&+\alpha(t,\omega_1)\alpha(t,\omega_2)\beta(t,\omega_1+\omega_2)\mathbb{E}[dV(\omega_1)dV(\omega_2)dU(\omega_1+\omega_2)]\\
&-\alpha(t,\omega_1)\alpha(t,\omega_2)\alpha(t,\omega_1+\omega_2)\mathbb{E}[dV(\omega_1)dV(\omega_2)dV(\omega_1+\omega_2)]\\
&=2\beta(t,\omega_1)\beta(t,\omega_2)\beta(t,\omega_1+\omega_2)\mathbb{R}B(\omega_1,\omega_2)d\omega_1 d\omega_2\\
&+2\beta(t,\omega_1)\beta(t,\omega_2)\alpha(t,\omega_1+\omega_2)\mathbb{I}B(\omega_1,\omega_2)d\omega_1 d\omega_2\\
&-2\beta(t,\omega_1)\alpha(t,\omega_2)\beta(t,\omega_1+\omega_2)\mathbb{I}B(\omega_1,\omega_2)d\omega_1 d\omega_2\\
&-2\alpha(t,\omega_1)\beta(t,\omega_2)\beta(t,\omega_1+\omega_2)\mathbb{I}B(\omega_1,\omega_2)d\omega_1 d\omega_2\\
&+2\beta(t,\omega_1)\alpha(t,\omega_2)\alpha(t,\omega_1+\omega_2)\mathbb{R}B(\omega_1,\omega_2)d\omega_1 d\omega_2\\
&+2\alpha(t,\omega_1)\beta(t,\omega_2)\alpha(t,\omega_1+\omega_2)\mathbb{R}B(\omega_1,\omega_2)d\omega_1 d\omega_2\\
&-2\alpha(t,\omega_1)\alpha(t,\omega_2)\beta(t,\omega_1+\omega_2)\mathbb{R}B(\omega_1,\omega_2)d\omega_1 d\omega_2\\
&-2\alpha(t,\omega_1)\alpha(t,\omega_2)\alpha(t,\omega_1+\omega_2)\mathbb{I}B(\omega_1,\omega_2)d\omega_1 d\omega_2\\
&=2A^*(t,\omega_1)A^*(t,\omega_2)A(t,\omega_1+\omega_2)\mathbb{E}[dZ^*(\omega_1)dZ^*(\omega_2)dZ^*(\omega_1+\omega_2)]\\
&=2B(t,\omega_1,\omega_2)d\omega_1 d\omega_2
\end{aligned}
\tag{A.6}
$$

## Appendix B. Ensemble properties

Here, we show that the expansion in Eq. (27) satisfies the necessary ensemble properties in 1st-order (mean), 2nd-order (variance) and 3rd-order respectively

### B.1. Mean

The processes are assumed to be of zero-mean, $\mathbb{E}[X(t)] = 0$. Since expectation is commutative over summation

$$\begin{aligned}\mathbb{E}[X(t)] &= \mathbb{E}[\sqrt{2}\sum_{k=0}^{N-1}[2S_p(t,\omega_k)\Delta\omega]^{\frac{1}{2}}\cos(\omega_k t+\phi_k)\\ &+\sqrt{2}\sum_{k=0}^{N-1}\sum_{i+j=k}^{i\geq j\geq 0}[2S(t,\omega_k)\Delta\omega]^{\frac{1}{2}}b_p(t,\omega_i,\omega_j)\cos(\omega_k t+\phi_i+\phi_j+\beta(t,\phi_i,\phi_j))]\\ &=\sqrt{2}\sum_{k=0}^{N-1}[2S_p(t,\omega_k)\Delta\omega]^{\frac{1}{2}}\mathbb{E}[\cos(\omega_k t+\phi_k)]\\ &+\sqrt{2}\sum_{k=0}^{N-1}\sum_{i+j=k}^{i\geq j\geq 0}[2S(t,\omega_k)\Delta\omega]^{\frac{1}{2}}b_p(t,\omega_i,\omega_j)\mathbb{E}[cos(\omega_k t+\phi_i+\phi_j+\beta(t,\phi_i,\phi_j))]\end{aligned} \tag{B.1}$$

Computing the expectation of $\cos(\omega_k t+\phi_k)$ and $\cos(\omega_k t+\phi_i+\phi_j+\beta(t,\omega_i,\omega_j))$ we have

$$\mathbb{E}[\cos(\omega_k t+\phi_k)] = \int_{-\infty}^{\infty} p_{\phi_k}\cos(\omega_k t+\phi_k)d\phi_k = \frac{1}{2\pi}\int_0^{2\pi}\cos(\omega_k t+\phi_k)d\phi_k = 0 \tag{B.2}$$

$$\begin{aligned}\mathbb{E}[\cos(\omega_k t+\phi_i+\phi_j+\beta(t,\omega_i,\omega_j))] &= \int_{-\infty}^{\infty}\int_{-\infty}^{\infty} p_{\phi_i}p_{\phi_j}\cos(\omega_k t+\phi_i+\phi_j+\beta(t,\omega_i,\omega_j))d\phi_i d\phi_j\\ &= \frac{1}{4\pi^2}\int_0^{2\pi}\int_0^{2\pi}\cos(\omega_k t+\phi_i+\phi_j+\beta(t,\omega_i,\omega_j))d\phi_i d\phi_j = 0\end{aligned} \tag{B.3}$$

Using the above results, we can conclude that

$$\mathbb{E}[X(t)] = 0 \tag{B.4}$$

### B.2. 2-point correlation function

The 2-point correlation function can be computed as

$$\begin{aligned}&R_2(t,t+\tau) = \mathbb{E}[X(t)X(t+\tau)]\\ &=\mathbb{E}[(\sqrt{2}\sum_{c=0}^{N-1}[2S_p(t,\omega_c)\Delta\omega]^{\frac{1}{2}}\cos(\omega_c t+\phi_c)\\ &+\sqrt{2}\sum_{c=0}^{N-1}\sum_{a+b=c}^{a\geq b\geq 0}[2S(t,\omega_c)\Delta\omega]^{\frac{1}{2}}b_p(t,\omega_a,\omega_b)\cos(\omega_c t+\phi_a+\phi_b+\beta(t,\phi_a,\phi_b))\\ &(\sqrt{2}\sum_{k=0}^{N-1}[2S_p(t+\tau,\omega_k)\Delta\omega]^{\frac{1}{2}}\cos(\omega_k(t+\tau)+\phi_k)\\ &+\sqrt{2}\sum_{k=0}^{N-1}\sum_{i+j=k}^{i\geq j\geq 0}[2S(t+\tau,\omega_k)\Delta\omega]^{\frac{1}{2}}b_p(t+\tau,\omega_i,\omega_j)\cos(\omega_k(t+\tau)+\phi_i+\phi_j+\beta(t+\tau,\phi_i,\phi_j)))]\\ &=4\mathbb{E}[\sum_{c=0}^{N-1}\sum_{k=0}^{N-1}\sqrt{S_p(t,\omega_c)S_p(t+\tau,\omega_k)}\Delta\omega\cos(\omega_c t+\phi_c)\cos(\omega_k(t+\tau)+\phi_k)\\ &+\sum_{k=0}^{N-1}\sum_{c=0}^{N-1}\sum_{a+b=c}^{a\geq b\geq 0}\sqrt{S(t+\tau,\omega_k)S(t,\omega_c)}b_p(t,\omega_a,\omega_b)\Delta\omega\\ &\cos(\omega_k(t+\tau)+\phi_k)\cos(\omega_c t+\phi_a+\phi_b+\beta(t,\phi_a,\phi_b))\\ &+\sum_{c=0}^{N-1}\sum_{k=0}^{N-1}\sum_{i+j=k}^{i\geq j\geq 0}\sqrt{S_p(t,\omega_c)S(t+\tau,\omega_k)}b_p(t+\tau,\omega_i,\omega_j)\Delta\omega\\ &\cos(\omega_c t+\phi_c)\cos(\omega_k(t+\tau)+\phi_i+\phi_j+\beta(t+\tau,\phi_i,\phi_j)))\\ &+\sum_{c=0}^{N-1}\sum_{k=0}^{N-1}\sum_{a+b=c}^{a\geq b\geq 0}\sum_{i+j=k}^{i\geq j\geq 0}\sqrt{S(t,\omega_c)S(t+\tau,\omega_k)}b_p(t,\omega_a,\omega_b)b_p(t+\tau,\omega_i,\omega_j)\Delta\omega\end{aligned}$$

$$
\begin{aligned}
&\cos(\omega_c t + \phi_a + \phi_b + \beta(t,\phi_a,\phi_b))\cos(\omega_k(t+\tau) + \phi_i + \phi_j + \beta(t+\tau,\phi_i,\phi_j))] \\
&= 2[\sum_{k=0}^{N-1}\sqrt{S_p(t,\omega_k)S_p(t+\tau,\omega_k)}\Delta\omega\cos(\omega_k\tau) \\
&+ \sum_{k=0}^{N-1}\sum_{i+j=k}^{i\geq j\geq 0}\sqrt{S(t,\omega_k)S(t+\tau,\omega_k)}b_p(t,\omega_a,\omega_b)b_p(t+\tau,\omega_i,\omega_j)\Delta\omega\cos(\omega_k\tau)] \\
&= 2\sum_{k=0}^{N-1}[\sqrt{S_p(t,\omega_k)S_p(t+\tau,\omega_k)}\Delta\omega\cos(\omega_k\tau) \\
&+ \sum_{i+j=k}^{i\geq j\geq 0}\sqrt{S(t,\omega_k)S(t+\tau,\omega_k)}b_p(t,\omega_i,\omega_j)b_p(t+\tau,\omega_i,\omega_j)\Delta\omega\cos(\omega_k\tau + \beta(t+\tau,\phi_i,\phi_j) - \beta(t,\phi_i,\phi_j))]
\end{aligned}
\tag{B.5}
$$

Substituting the value of $\tau = 0$ i.e. computing the variance at time $t$,

$$
\begin{aligned}
R(t,t) &= E[X^2(t)] = 2\sum_{k=0}^{N-1}S(t,\omega_k)\Delta\omega \\
R(t,t) &= E[X^2(t)] = \int_{-\infty}^{\infty}S(t,\omega)d\omega
\end{aligned}
\tag{B.6}
$$

we see that the process has variance equal to the integral of the evolutionary spectrum, as expected. This is equivalent to the variance function from the 2nd-order SRM [32].

### *B.3. 3-point correlation function*

The 3-point correlation function can be computed as

$$
\begin{aligned}
&R_3(t,t+\tau_1,t+\tau_2) = \mathbb{E}[X(t)X(t+\tau_1)X(t+\tau_2)] \\
&= \mathbb{E}[(\sqrt{2}\sum_{c=0}^{N-1}[2S_p(t,\omega_c)\Delta\omega]^{\frac{1}{2}}\cos(\omega_c t + \phi_c) \\
&+ \sqrt{2}\sum_{c=0}^{N-1}\sum_{a+b=c}^{a\geq b\geq 0}[2S(t,\omega_c)\Delta\omega]^{\frac{1}{2}}b_p(t,\omega_a,\omega_b)\cos(\omega_c t + \phi_a + \phi_b + \beta(t,\phi_a,\phi_b))) \\
&(\sqrt{2}\sum_{k=0}^{N-1}[2S_p(t+\tau_1,\omega_k)\Delta\omega]^{\frac{1}{2}}\cos(\omega_k(t+\tau_1) + \phi_k) \\
&+ \sqrt{2}\sum_{k=0}^{N-1}\sum_{i+j=k}^{i\geq j\geq 0}[2S(t+\tau_1,\omega_k)\Delta\omega]^{\frac{1}{2}}b_p(t+\tau_1,\omega_i,\omega_j)\cos(\omega_k(t+\tau_1) + \phi_i + \phi_j + \beta(t+\tau_1,\phi_i,\phi_j))) \\
&(\sqrt{2}\sum_{z=0}^{N-1}[2S_p(t+\tau_2,\omega_z)\Delta\omega]^{\frac{1}{2}}\cos(\omega_z(t+\tau_2) + \phi_z) \\
&+ \sqrt{2}\sum_{z=0}^{N-1}\sum_{x+y=z}^{x\geq y\geq 0}[2S(t+\tau_2,\omega_z)\Delta\omega]^{\frac{1}{2}}b_p(t+\tau_2,\omega_x,\omega_y)\cos(\omega_z(t+\tau_2) + \phi_x + \phi_y + \beta(t+\tau_2,\phi_x,\phi_y)))]
\end{aligned}
\tag{B.7}
$$

which simplifies to

$$
\begin{aligned}
&R_3(t,t+\tau_1,t+\tau_2) = \\
&2(\Delta\omega)^{3/2}[\sum_{k=0}^{N-1}\sum_{i+j=k}^{i\geq j\geq 0}\sqrt{S_p(t,\omega_i)S_p(t+\tau_1,\omega_j)S(t+\tau_2,\omega_k)}b_p(t+\tau_2,\omega_i,\omega_j)\cos(\omega_k\tau_2 + \beta(t+\tau_2,\phi_i,\phi_j) - \omega_j\tau_1) \\
&+ \sqrt{S_p(t+\tau_1,\omega_i)S_p(t,\omega_j)S(t+\tau_2,\omega_k)}b_p(t+\tau_2,\omega_i,\omega_j)\cos(\omega_k\tau_2 + \beta(t+\tau_2,\phi_i,\phi_j) - \omega_i\tau_1) \\
&+ \sqrt{S_p(t+\tau_2,\omega_i)S_p(t,\omega_j)S(t+\tau_1,\omega_k)}b_p(t+\tau_1,\omega_i,\omega_j)\cos(\omega_k\tau_1 + \beta(t+\tau_1,\phi_i,\phi_j) - \omega_i\tau_2) \\
&+ \sqrt{S_p(t,\omega_i)S_p(t+\tau_2,\omega_j)S(t+\tau_1,\omega_k)}b_p(t+\tau_1,\omega_i,\omega_j)\cos(\omega_k\tau_1 + \beta(t+\tau_1,\phi_i,\phi_j) - \omega_j\tau_2) \\
&+ \sqrt{S_p(t+\tau_1,\omega_i)S_p(t+\tau_2,\omega_j)S(t,\omega_k)}b_p(t,\omega_i,\omega_j)\cos(\beta(t,\phi_i,\phi_j) - \omega_i\tau_1 - \omega_j\tau_2) \\
&+ \sqrt{S_p(t+\tau_2,\omega_i)S_p(t+\tau_1,\omega_j)S(t,\omega_k)}b_p(t,\omega_i,\omega_j)\cos(\beta(t+\tau_2,\phi_i,\phi_j) - \omega_i\tau_2 - \omega_j\tau_1)]
\end{aligned}
\tag{B.8}
$$

Substituting $\tau_1 = \tau_2 = 0$, i.e. computing the 3-order correlation function at time $t$,

$$R_3(t,t,t) = 12(\Delta\omega)^{3/2} \sum_{k=0}^{N-1} \sum_{i+j=k}^{i\geq j\geq 0} \sqrt{S_p(t,\omega_i)S_p(t,\omega_j)S(t,\omega_k)} b_p(t,\omega_i,\omega_j)\cos(\beta(t,\phi_i,\phi_j)) \tag{B.9}$$

Plugging in the value of $b_p(t,\omega_1,\omega_2)$, yields

$$\begin{aligned} R_3(t,t,t) &= E[X^3(t)] = 12(\Delta\omega)^2 \sum_{k=0}^{N-1} \sum_{i+j=k}^{i\geq j\geq 0} B(t,\omega_i,\omega_j) \\ R_3(t,t,t) &= E[X^3(t)] = \int_{-\infty}^{\infty} B(t,\omega_i,\omega_j) d\omega_1 d\omega_2, \end{aligned} \tag{B.10}$$

which is consistent with the fact that the integral of the evolutionary bispectrum is equal to the third moment of the process at time $t$ as shown in Appendix C.

## Appendix C. Evolutionary bispectrum as the distribution of skewness

Here, we show that the proposed evolutionary bispectrum, when integrated over frequency pairs $\omega_1, \omega_2$, yields the third-moment of the process at a given time $t$.

First, consider the three-point correlation given by

$$\begin{aligned} R_3(s,t,u) &= \mathbb{E}\left[\int_{-\infty}^{\infty}\int_{-\infty}^{\infty}\int_{-\infty}^{\infty} A(s,\omega_1)dZ(\omega_1)A(t,\omega_2)dZ(\omega_2)A(u,\omega_3)dZ(\omega_3)\right] \\ &= \int_{-\infty}^{\infty}\int_{-\infty}^{\infty}\int_{-\infty}^{\infty} A(s,\omega_1)A(t,\omega_2)A(u,\omega_3)\mathbb{E}\left[dZ(\omega_1)dZ(\omega_2)dZ(\omega_3)\right] \end{aligned} \tag{C.1}$$

Next, consider the third-order orthogonality conditions of the spectral process, here repeated from Eq. (13)

$$\begin{aligned} &\mathbb{E}[dZ(\omega_1)dZ(\omega_2)dZ(\omega_3)] = B(\omega_1,\omega_2)d\omega_1 d\omega_2 \qquad \text{if} \quad \omega_1+\omega_2-\omega_3 = 0 \\ &\mathbb{E}[dZ(\omega_1)dZ(\omega_2)dZ(\omega_3)] = 0 \qquad\qquad\qquad\qquad\qquad\quad \text{otherwise} \end{aligned} \tag{C.2}$$

Applying these orthogonality conditions and considering the third moment of a point at time $t$ yields

$$\begin{aligned} R_3(s,t,u) &= \int_{-\infty}^{\infty}\int_{-\infty}^{\infty} A(s,\omega_1)A(t,\omega_2)A(u,\omega_1+\omega_2)\mathbb{E}[dZ(\omega_1)dZ(\omega_2)dZ^*(\omega_1+\omega_2)] \\ R_3(t,t,t) &= E[X^3(t)] = \int_{-\infty}^{\infty}\int_{-\infty}^{\infty} A(t,\omega_1)A(t,\omega_2)A(t,\omega_1+\omega_2)B(\omega_1,\omega_2)d\omega_1 d\omega_2 \end{aligned} \tag{C.3}$$

Finally, we recognize that the integrand is the proposed evolutionary bispectrum such that

$$E[X^3(t)] = \int_{-\infty}^{\infty}\int_{-\infty}^{\infty} B(t,\omega_1,\omega_2)d\omega_1 d\omega_2, \tag{C.4}$$

which is related to the skewness, $\gamma_3$ through

$$\gamma_3 = \frac{\mathbb{E}[X^3(t)]}{(\mathbb{E}[X^2(t)])^{3/2}} \tag{C.5}$$

## Appendix D. Theoretical reconstruction of decomposed spectral quantities

### D.1. Pure component of the variance

From the orthogonal projection in Eq. (38), we have

$$\sqrt{S_p(t,\omega)} = \sum_{q=1}^{N_q} a_q(t)\Phi_q(\omega) \tag{D.1}$$

The square of the above equation yields

$$S_p(t,\omega) = \sum_{q_1=1}^{N_q}\sum_{q_2=1}^{N_q} a_{q_1}(t)\Phi_{q_1}(\omega)a_{q_2}(t)\Phi_{q_2}(\omega) \tag{D.2}$$

Taking the sum of along the range of the frequency terms yields

$$\sum_{k=0}^{N_\omega-1} S_p(t,\omega_k) = \sum_{k=0}^{N_\omega-1}\sum_{q_1=1}^{N_q}\sum_{q_2=1}^{N_q} a_{q_1}(t)\Phi_{q_1}(\omega_k)a_{q_2}(t)\Phi_{q_2}(\omega_k) \tag{D.3}$$

Since $\Phi_q(\omega)$ are orthogonal vectors, the following equation holds

$$\sum_{k=1}^{N_\omega} \Phi_{q_1}(\omega_k)\Phi_{q_2}(\omega_k) = \begin{cases} 1, \text{if } q_1 = q_2 \\ 0, \text{otherwise} \end{cases} \tag{D.4}$$

Substituting the above orthogonality condition into Eq. (D.3) yields

$$\begin{aligned} \sum_{k=1}^{N_\omega} S_p(t,\omega_k) &= \sum_{q=1}^{N_q} a_q^2(t) \sum_{k=1}^{N_\omega} \Phi_q^2(\omega_k) \\ \sum_{k=1}^{N_\omega} S_p(t,\omega_k) &= \sum_{q=1}^{N_q} a_q^2(t) \end{aligned} \tag{D.5}$$

The variance of the pure component of the non-stationary process $X(t)$ can then be written as

$$Var[X_p(t)] = 2\Delta\omega \sum_{k=1}^{N_\omega} S_p(t,\omega_k) = 2\Delta\omega \sum_{q=1}^{N_q} a_q^2(t), \tag{D.6}$$

which illustrates that $a_q(t)$ can be interpreted as modulating the pure component of the variance.

### D.2. Interactive component of the variance

Consider the decomposition of the bispectrum from Eq. (37)

$$\frac{|B(t,\omega_i,\omega_j)|}{\sqrt{S_p(t,\omega_i)S_p(t,\omega_j)}} = \sum_{r=1,s=1}^{N_q,N_q} |b_{rs}(t)|\theta_{rs}(\omega_i,\omega_j) = \sum_{r=1,s=1}^{N_q,N_q} b_{rs}(t)\Phi_r(\omega_i)\Phi_s(\omega_j) \tag{D.7}$$

The square of the above equation yields

$$\frac{|B(t,\omega_i,\omega_j)|^2}{S_p(t,\omega_i)S_p(t,\omega_j)} = \sum_{r_1=1,s_1=1}^{N_q,N_q} \sum_{r_2=1,s_2=1}^{N_q,N_q} |b_{r_1s_1}(t)|\theta_{r_1s_1}(\omega_i,\omega_j)|b_{r_2s_2}(t)|\theta_{r_2s_2}(\omega_i,\omega_j) \tag{D.8}$$

Taking the sums of the term along the frequency range yields

$$\begin{aligned} \sum_{k=1}^{N_\omega} \sum_{i+j=k}^{i\geq 0,j\geq 0} \frac{|B(t,\omega_i,\omega_j)|^2}{S_p(t,\omega_i)S_p(t,\omega_j)} &= \sum_{i+j=k}^{i\geq 0,j\geq 0} \sum_{r_1=1,s_1=1}^{N_q,N_q} \sum_{r_2=1,s_2=1}^{N_q,N_q} |b_{r_1s_1}(t)|\theta_{r_1s_1}(\omega_i,\omega_j)|b_{r_2s_2}(t)|\theta_{r_2s_2}(\omega_i,\omega_j) \\ &= \sum_{k=1}^{N_\omega} \sum_{i+j=k}^{i\geq 0,j\geq 0} \sum_{r_1=1,s_1=1}^{N_q,N_q} \sum_{r_2=1,s_2=1}^{N_q,N_q} |b_{r_1s_1}(t)|\Phi_{r_1}(\omega_i)\Phi_{s_1}(\omega_j)|b_{r_2s_2}(t)|\Phi_{r_2}(\omega_i)\Phi_{s_2}(\omega_j) \\ &= \sum_{r_1=1,s_1=1}^{N_q,N_q} \sum_{r_2=1,s_2=1}^{N_q,N_q} |b_{r_1s_1}(t) \parallel b_{r_2s_2}(t)| \sum_{k=1}^{N_\omega} \sum_{i+j=k}^{i\geq 0,j\geq 0} \Phi_{r_1}(\omega_i)\Phi_{s_1}(\omega_j)\Phi_{r_2}(\omega_i)\Phi_{s_2}(\omega_j) \\ &= \sum_{r_1=1,s_1=1}^{N_q,N_q} \sum_{r_2=1,s_2=1}^{N_q,N_q} |b_{r_1s_1}(t)||b_{r_2s_2}(t)| \sum_{k=1}^{N_\omega} \sum_{i+j=k}^{i\geq 0,j\geq 0} \Phi_{r_1}(\omega_i)\Phi_{r_2}(\omega_i)\Phi_{s_1}(\omega_j)\Phi_{s_2}(\omega_j) \end{aligned} \tag{D.9}$$

We have the orthogonality condition of the singular vectors

$$\sum_{i=1,j=1}^{N_\omega,N_\omega} \Phi_{r_1}(\omega_i)\Phi_{r_2}(\omega_i)\Phi_{s_1}(\omega_j)\Phi_{s_2}(\omega_j) = \begin{cases} 1, \text{if } r_1 = r_2, s_1 = s_2 \\ 0, \text{otherwise} \end{cases} \tag{D.10}$$

Assuming that most of the information in the singular vectors is contained in the lower frequency ranges, the following approximation holds

$$\sum_{k=1}^{N_\omega} \sum_{i+j=k}^{i\geq 0,j\geq 0} \Phi_{r_1}(\omega_i)\Phi_{r_2}(\omega_i)\Phi_{s_1}(\omega_j)\Phi_{s_2}(\omega_j) \simeq \begin{cases} 1, \text{if } r_1 = r_2, s_1 = s_2 \\ 0, \text{otherwise} \end{cases} \tag{D.11}$$

Substituting this orthogonality condition into Eq. (D.9) yields

$$\sum_{k=1}^{N_\omega} \sum_{i+j=k}^{i\geq 0,j\geq 0} \frac{|B(t,\omega_i,\omega_j)|^2}{S_p(t,\omega_i)S_p(t,\omega_j)} = \sum_{r=1,s=1}^{N_q,N_q} |b_{rs}(t)|^2 \tag{D.12}$$

The variance of the interactive component of the non-stationary process $X(t)$ can be written as

$$Var[X_I(t)] = \Delta\omega^2 \sum_{k=1}^{N_\omega} \sum_{i+j=k}^{i\geq 0,j\geq 0} \frac{|B(t,\omega_i,\omega_j)|^2}{S_p(t,\omega_i)S_p(t,\omega_j)} = \Delta\omega^2 \sum_{r=1,s=1}^{N_q,N_q} |b_{rs}(t)|^2, \tag{D.13}$$

which confirms that $b_{rs}(t)$ modulates the variance associated with wave interactions.

### D.3. Third moment

The bispectrum can be represented as

$$\begin{aligned} B(t,\omega_i,\omega_j) &= \frac{B(t,\omega_i,\omega_j)}{\sqrt{S_p(t,\omega_i)S_p(t,\omega_j)}}\sqrt{S_p(t,\omega_i)}\sqrt{S_p(t,\omega_j)} \\ &= \sum_{r=1,s=1}^{N_q,N_q} b_{rs}(t)\theta_{rs}(\omega_i,\omega_j)\sum_{q_1=1}^{N_{q_1}} a_{q_1}(t)\Phi_{q_1}(\omega_i)\sum_{q_2=1}^{N_{q_2}} a_{q_2}(t)\Phi_{q_2}(\omega_j) \\ &= \sum_{r=1,s=1}^{N_q,N_q}\sum_{q_1=1}^{N_q}\sum_{q_2=1}^{N_q} b_{rs}(t)a_{q_1}(t)a_{q_2}(t)\Phi_{q_1}(\omega_i)\Phi_r(\omega_i)\Phi_{q_2}(\omega_j)\Phi_s(\omega_j) \end{aligned} \tag{D.14}$$

Taking the sum of the bispectrum over the frequency domain yields

$$\begin{aligned} \sum_{k=1}^{N_\omega}\sum_{i+j=k}^{i\geq 0,j\geq 0} B(t,\omega_i,\omega_j) &= \sum_{k=1}^{N_\omega}\sum_{i+j=k}^{i\geq 0,j\geq 0}\sum_{r=1,s=1}^{N_q,N_q}\sum_{q_1=1}^{N_q}\sum_{q_2=1}^{N_q} b_{rs}(t)a_{q_1}(t)a_{q_2}(t)\Phi_{q_1}(\omega_i)\Phi_r(\omega_i)\Phi_{q_2}(\omega_j)\Phi_s(\omega_j) \\ \sum_{k=1}^{N_\omega}\sum_{i+j=k}^{i\geq 0,j\geq 0} B(t,\omega_i,\omega_j) &= \sum_{r=1,s=1}^{N_q,N_q}\sum_{q_1=1}^{N_q}\sum_{q_2=1}^{N_q} b_{rs}(t)a_{q_1}(t)a_{q_2}(t)\sum_{k=1}^{N_\omega}\sum_{i+j=k}^{i\geq 0,j\geq 0}\Phi_{q_1}(\omega_i)\Phi_r(\omega_i)\Phi_{q_2}(\omega_j)\Phi_s(\omega_j) \end{aligned} \tag{D.15}$$

The orthogonality conditions in this scenario are

$$\sum_{k=1}^{N_\omega}\sum_{i+j=k}^{i\geq 0,j\geq 0}\Phi_r(\omega_i)\Phi_{q_1}(\omega_i)\Phi_s(\omega_j)\Phi_{q_2}(\omega_j) \simeq \begin{cases} 1, \text{if } q_1 = r, q_2 = s \\ 0, \text{otherwise} \end{cases} \tag{D.16}$$

Substituting the orthogonality conditions into the above equation yields

$$\sum_{k=1}^{N_\omega}\sum_{i+j=k}^{i\geq 0,j\geq 0} B(t,\omega_i,\omega_j) = \sum_{r=1,s=1}^{N_q,N_q} b_{rs}(t)a_r(t)a_s(t) \tag{D.17}$$

The definition of the third moment of the process is

$$\begin{aligned} E[X^3(t)] &= 6\sum_{k=1}^{N_\omega}\sum_{i+j=k}^{i\geq 0,j\geq 0}\mathrm{Re}(B(t,\omega_i,\omega_j))\Delta\omega^2 \approx 6\sum_{r=1,s=1}^{N_q,N_q}\mathrm{Re}(b_{rs}(t))a_r(t)a_s(t)\Delta\omega^2 \\ &= 6\sum_{r=1,s=1}^{N_q,N_q}|b_{rs}(t)|a_r(t)a_s(t)\cos(\gamma_{rs}(t))\Delta\omega^2 \end{aligned} \tag{D.18}$$

## Appendix E. Ensemble properties of POD formula

Here, we show that the expansion Eq. (40) satisfies the necessary ensemble properties in 2nd-order (variance) and 3rd-order respectively as presented in Appendix D.

### E.1. 2-point correlation function

The ensemble 2nd-order properties of the pure and interactive components of the (expansion are investigated separately.

#### E.1.1. Pure component

The variance of the pure component of the process can be expanded as

$$Var_p[X(t)] = 4\mathbb{E}[\Delta\omega\sum_{k_1}\sum_{r_1}\sum_{q_2}\sum_{r_2} a_{r_1}(t)a_{r_2}(t)\Phi_{r_1}(\omega_{k_1})\Phi_{r_2}(\omega_{k_2})\Delta\omega\cos(\omega_{k_1}t-\phi_{r_1k_1})\cos(\omega_{k_2}t-\phi_{r_2k_2})] \tag{E.1}$$

and we know that

$$\mathbb{E}[\cos(\omega_{k_1}t-\phi_{r_1k_1})\cos(\omega_{k_2}t-\phi_{r_2k_2})] = \begin{cases} \frac{1}{2}, \text{if } r_1 = r_2, k_1 = k_2 \\ 0, \text{otherwise} \end{cases} \tag{E.2}$$

Substituting these values into the ensemble equation yields

$$\begin{aligned} Var_p[X(t)] &= 2\Delta\omega\sum_k\sum_r a_r(t)a_r(t)\Phi_r(\omega_k)\Phi_r(\omega_k) \\ &= 2\Delta\omega\sum_k\sum_r a_r^2(t)\Phi_r^2(\omega_k) = 2\Delta\omega\sum_r a_r^2(t) \end{aligned} \tag{E.3}$$

which is the equal to the theoretical value Eq. (D.6).

*E.1.2. Interactive component*

The variance of the interactive component of the process can be expanded as

$$Var_I[X(t)] = 4\mathbb{E}[\sum_{k_1}\sum_{k_2}\sum_{r_1}\sum_{s_1}\sum_{r_2}\sum_{s_2}\sum_{i_1+j_1=k_1}^{i_1\geq j_1\geq 0}\sum_{i_2+j_2=k_2}^{i_2\geq j_2\geq 0}|b_{r_1s_1}(t)||b_{r_2s_2}(t)| \\ \Phi_{r_1}(\omega_{i_1})\Phi_{r_2}(\omega_{i_2})\Phi_{s_1}(\omega_{j_1})\Phi_{s_2}(\omega_{j_2})\Delta\omega^2\cos(\omega_{k_1}t-\phi_{r_1i_1}-\phi_{s_1j_1}+\gamma_{r_1s_1}(t))\cos(\omega_{k_1}t-\phi_{r_2i_2}-\phi_{s_2j_2}+\gamma_{r_2s_2}(t))] \tag{E.4}$$

and we know that

$$\mathbb{E}[\cos(\omega_{k_1}t-\phi_{r_1i_1}-\phi_{s_1j_1}++\gamma_{r_1s_1}(t))\cos(\omega_{k_1}t-\phi_{r_2i_2}-\phi_{s_2j_2}++\gamma_{r_2s_2}(t))] = \\ \begin{cases}\frac{1}{2}, \text{if } r_1=r_2, s_1=s_2, i_1=i_2, j_1=j_2, k_1=k_2\\ 0, \text{otherwise}\end{cases} \tag{E.5}$$

Substituting the values in the ensemble equation yields

$$\begin{aligned} Var_I[X(t)] &= 2\sum_k\sum_r\sum_s\sum_{i+j=k}^{i\geq j\geq 0}|b_{rs}(t)|^2\Phi_r^2(\omega_i)\Phi_s^2(\omega_j)\Delta\omega^2 \\ &= \sum_r\sum_s b_{rs}^2(t)\Delta\omega^2\sum_k\sum_{i+j=k}^{i\geq 0,j\geq 0}\Phi_r^2(\omega_i)\Phi_s^2(\omega_j) \\ &= \sum_r\sum_s|b_{rs}(t)|^2\Delta\omega^2 \end{aligned} \tag{E.6}$$

which is the equal to the theoretical value Eq. (D.13)

*E.2. Third moment*

The third moment of the process can be expanded as

$$\mathbb{E}[X^3(t)] = 48\mathbb{E}[\sum_{k_1}\sum_{k_2}\sum_{k_3}\sum_p\sum_q\sum_r\sum_s\sum_{i_3+j_3=k_3}^{i_3\geq j_3\geq 0}a_p(t)\Phi_p(\omega_{k_1})a_q(t)\Phi_q(\omega_{k_2})|b_{rs}(t)| \\ \theta_{rs}(\omega_{i_3},\omega_{j_3})\Delta\omega^2\cos(\omega_{k_1}t-\phi_{pk_1})\cos(\omega_{k_2}t-\phi_{qk_2})\cos(\omega_{k_3}t-\phi_{ri_3}-\phi_{sj_3}+\gamma_{rs}(t))] \tag{E.7}$$

and we know that

$$\mathbb{E}[\cos(\omega_{k_1}t-\phi_{pk_1})\cos(\omega_{k_2}t-\phi_{qk_2})\cos(\omega_{k_3}t-\phi_{ri_3}-\phi_{sj_3}+\gamma_{rs}(t))] = \\ \begin{cases}\frac{1}{4}\cos(\gamma_{rs}(t)), \text{if } p=r, q=s, k_1=i_3, k_2=j_3\\ 0, \text{otherwise}\end{cases} \tag{E.8}$$

Substituting this expectation into the ensemble equation yields

$$\begin{aligned} \mathbb{E}[X^3(t)] &= 12\sum_k\sum_r\sum_s\sum_{i+j=k}^{i\geq j\geq 0}a_r(t)\Phi_r(\omega_i)a_s(t)\Phi_s(\omega_j)|b_{rs}(t)|\cos(\gamma_{rs}(t))\Phi_r(\omega_i)\Phi_s(\omega_j)\Delta\omega^2 \\ &= 6\sum_r\sum_s a_r(t)a_s(t)|b_{rs}(t)|\cos(\gamma_{rs}(t))\Delta\omega^2 \end{aligned} \tag{E.9}$$

which is the same as Eq. (D.18)

## References


[1] S.P. Huang, S.T. Quek, K.K. Phoon, Convergence study of the truncated Karhunen–Loeve expansion for simulation of stochastic processes, Internat. J. Numer. Methods Engrg. 52 (9) (2001) 1029–1043.
[2] M. Shinozuka, Monte Carlo Solution of structural dynamics, Comput. Struct. 2 (1972) 855–874.
[3] J.-N. Yang, Simulation of random envelope processes, J. Sound Vib. 21 (1) (1972) 73–85.
[4] G. Deodatis, Simulation of ergodic multivariate stochastic processes, J. Eng. Mech. 122 (8) (1996) 778–787.
[5] G. Deodatis, M. Shinozuka, Simulation of seismic ground motion using stochastic waves, J. Eng. Mech. 115 (12) (1989) 2723–2737.
[6] M. Shinozuka, G. Deodatis, Simulation of multi-dimensional Gaussian stochastic fields by spectral representation, Appl. Mech. Rev. 49 (1) (1996) 29–53.
[7] M. Grigoriu, On the spectral representation method in simulation, Probab. Eng. Mech. 8 (2) (1993) 75–90.
[8] B. Puig, F. Poirion, C. Soize, Non-Gaussian simulation using Hermite polynomial expansion: Convergences and algorithms, Probab. Eng. Mech. 17 (3) (2002) 253–264.
[9] Z. Liu, Z. Liu, Y. Peng, Dimension reduction of Karhunen-Loeve expansion for simulation of stochastic processes, J. Sound Vib. 408 (2017) 168–189.
[10] M. Grigoriu, Simulation of stationary non-Gaussian translation processes, J. Eng. Mech. 124 (2) (1998) 121–126.
[11] M.D. Shields, G. Deodatis, P. Bocchini, A simple and efficient methodology to approximate a general non-Gaussian stationary stochastic process by a translation process, Probab. Eng. Mech. 26 (4) (2011) 511–519.
[12] M.D. Shields, G. Deodatis, A simple and efficient methodology to approximate a general non-Gaussian stationary stochastic vector process by a translation process with applications in wind velocity simulation, Probab. Eng. Mech. 31 (2013) 19–29.

[13] H. Kim, M.D. Shields, Modeling strongly non-Gaussian non-stationary stochastic processes using the iterative translation approximation method and Karhunen-Loève expansion, Comput. Struct. 161 (2015) 31–42.
[14] M.D. Shields, H. Kim, Simulation of higher-order stochastic processes by spectral representation, Probab. Eng. Mech. 47 (October 2016) (2017) 1–15.
[15] L. Vandanapu, M.D. Shields, 3rd-order spectral representation method: Simulation of multi-dimensional random fields and ergodic multi-variate random processes with fast Fourier transform implementation, Probab. Eng. Mech. 64 (October 2020) (2021) 103128.
[16] M. Priestley, Evolutionary spectra and non-stationary processes, J. R. Stat. Soc. Ser. B Stat. Methodol. 27 (2) (1965) 204–237.
[17] Y. Li, A. Kareem, Simulation of multivariate nonstationary random processes: Hybrid DFT and digital filtering approach, J. Eng. Mech. 123 (12) (1997) 1302–1310.
[18] G. Huang, An efficient simulation approach for multivariate nonstationary process: Hybrid of wavelet and spectral representation method, Probab. Eng. Mech. 37 (2014) 74–83.
[19] Y. Li, A. Kareem, Simulation of multivariate nonstationary random processes by FFT, J. Eng. Mech. 117 (5) (1991) 1037–1058.
[20] G. Huang, Application of proper orthogonal decomposition in fast Fourier transform—Assisted multivariate nonstationary process simulation, J. Eng. Mech. 141 (7) (2015) 04015015.
[21] L. Peng, G. Huang, X. Chen, A. Kareem, Simulation of multivariate nonstationary random processes: Hybrid stochastic wave and proper orthogonal decomposition approach, J. Eng. Mech. 143 (9) (2017) 1–16.
[22] S. Sakamoto, R. Ghanem, Simulation of multi-dimensional non-Gaussian non-stationary random fields, Probab. Eng. Mech. 17 (2) (2002) 167–176.
[23] F. Ferrante, L. Graham-Brady, Stochastic simulation of non-Gaussian/non-stationary properties in a functionally graded plate, Comput. Methods Appl. Mech. Engrg. 194 (12–16) (2005) 1675–1692.
[24] M. Shields, G. Deodatis, Estimation of evolutionary spectra for simulation of non-stationary and non-Gaussian stochastic processes, Comput. Struct. 126 (2013) 149–163.
[25] H. Dai, Z. Zheng, H. Ma, An explicit method for simulating non-Gaussian and non-stationary stochastic processes by Karhunen-Loève and polynomial chaos expansion, Mech. Syst. Signal Process. 115 (2019) 1–13.
[26] S. Montoya-Noguera, T. Zhao, Y. Hu, Y. Wang, K.-K. Phoon, Simulation of non-stationary non-Gaussian random fields from sparse measurements using Bayesian compressive sampling and Karhunen-Loève expansion, Struct. Saf. 79 (2019) 66–79.
[27] Z. Zheng, H. Dai, Y. Wang, W. Wang, A sample-based iterative scheme for simulating non-stationary non-Gaussian stochastic processes, Mech. Syst. Signal Process. 151 (2021) 107420.
[28] H. Cramer, Stationary and Related Stochastic Processes; Sample Function Properties and their Applications, Wiley, New York, 1967.
[29] M. Priestley, Power spectral analysis of non-stationary random processes, J. Sound Vib. 6 (1) (1967) 86–97.
[30] T.G. Kolda, B.W. Bader, Tensor decompositions and applications, SIAM Rev. 51 (3) (2009) 455–500.
[31] R.W. Clough, J. Penzien, Dynamics of Structures, (xxii, 634) McGraw-Hill, New York, 1975.
[32] J. Liang, S.R. Chaudhuri, M. Shinozuka, Simulation of nonstationary stochastic processes by spectral representation, J. Eng. Mech. 133 (6) (2007) 616–627.